Microporous and Mesoporous Materials 224 (2016) 360–371

Contents lists available at ScienceDirect

Microporous and Mesoporous Materials

journal homepage: www.elsevier.com/locate/micromeso

New insights on estimating pore size distribution of latex particles: Statistical mechanics approach and modeling

Manel Bergaoui [a], Mohamed Khalfaoui [a, b, *], Jhonny Villarroel-Rocha [c], Deicy Barrera [c], Shaheen Al-Muhtaseb [d], Eduardo Enciso [e], Karim Sapag [c], Abdelmottaleb Ben Lamine [a]

[a] Unité de Recherche de Physique Quantique, Département de Physique, Faculté des Sciences de Monastir, 5019, Université de Monastir, Tunisia
[b] Département de Technologie, Institut Supérieur d'Informatique et de Mathématiques de Monastir, Route de la Corniche, Monastir, 5000, Université de Monastir, Tunisia
[c] Laboratorio de Sólidos Porosos, Instituto de Física Aplicada, CONICET, Universidad Nacional de San Luis, Chacabuco 917, 5700, San Luis, Argentina
[d] Department of Chemical Engineering, Qatar University, P.O. Box 2713, Doha, Qatar
[e] Departamento de Química Física I, Facultad de Ciencias Químicas, Universidad Complutense, 28040, Madrid, Spain

ARTICLE INFO

Article history:
Received 19 October 2015
Accepted 24 November 2015
Available online 12 January 2016

Keywords:
Statistical mechanics approach
Pore size distribution
Sorption modeling
Nitrogen adsorption-desorption isotherms
Latex particles

ABSTRACT

New statistical mechanics approach for pore size distribution applied in wide the relative pressure range is proposed. The new proposed model was applied to nitrogen adsorption-desorption isotherms at 77 K onto five functionalized polystyrene latices. Results showed that the proposed model can reproduce all results found by traditional methods such as NLDFT, BJH and VBS where some of them can be applied only for a specific range of pore size. A segmentation procedure is adopted and it is shown that the corresponding algorithm can be successfully applied for determining pore size distributions over a wide range of pore size. When this method is applied an isotherms Type II and III (materials with larger mesopores and/or macropores) gives additional information that is not obtained with the other methods. The obtained results showed that the copolymerization plays an important role in the porosity and the specific surface area, whereas, the high polydispersity index, PDI, can reduce the porosity. The samples studied within the present work present small and large mesopores and even macropores as it is suggested by the new proposed model, and part of this porosity could be related to the interparticle and also to the intraparticle porosity.

1. Introduction

Numerous polystyrene-derived sorbents are widely used in modern technology as soap-free latex substrates for proteins. That is because the polystyrene latex is stable and particle sizes are monodispersed [1]. However, many studies have shown that bio-specific interactions can be developed between biological compounds and functionalized polystyrene particles with suitable chemical groups [2]. Furthermore, polystyrene and its copolymers gained popularity as excellent adsorbent for protein in vitro as well as in vivo [3]. Among the advantages of using polymer latices as adsorbents for proteins are the large surface area for adsorption and the physicochemical properties of a latex particle [4]. Then, the copolymerization was found to affect significantly the specific surface area of the porous monolith [5]. Moreover, the porosity of these materials is well known to result from micro-phase separation in the course of free radical copolymerization of the co-monomers [5]. This leads to the important role to use copolymers in protein adsorption. Furthermore, it is necessary to establish the porosity of these materials and then to deduce their specific surface area.

Among the different experimental techniques to characterize the porous structures of latex particles, the N_2 adsorption-desorption at 77 K was found to be an efficient tool to evaluate the pore size distribution (PSD) using several methods/models [6,7]. In this sense, many researchers have been developed different methods based on the capillary and molecular theories [8], named macroscopic and microscopic methods, respectively. Among the microscopic methods are the Molecular Dynamics (MD) [9] Monte Carlo (MC) [10] and the models based in the Density Functional Theory (DFT) [11–13]. On other hand, several authors have

* Corresponding author. Unité de Recherche de Physique Quantique, Département de Physique, Faculté des Sciences de Monastir 5019, Université de Monastir, Tunisia. Tel.: +216 73 464 168.
E-mail address: mohamed_khalfaoui@yahoo.com (M. Khalfaoui).

http://dx.doi.org/10.1016/j.micromeso.2015.11.040
1387-1811/

Nomenclature

ARE	Absolute relative error
D_n	Number-average diameter(nm)
D_m	Mass average diameter(nm)
D_i	Diameter of particle (nm)
ERRSQ	Sum of the squares of the errors
$f(w)$	Pore size distribution (PSD) function (nm^{-1})
f_c	Correction term (nm)
j	Number of data points
h	Planck's constant ($6.626 \times 10^{-34} m^2 kg/s$)
$\mathscr{K}$	Characteristic constant for a defined adsorbate/adsorbent system (kJ.nm/mol)
k_B	Boltzmann's constant ($1.380 \times 10^{-23} m^2 kg/s.K$)
$\mathscr{M}$	Adsorbed molecule(s)
m	Mass of an adsorbed molecule (g)
N	Number of adsorbate molecules
n	Number of adsorbed molecule(s) per site S
N_m	Receptor site densities ($\mu g/cm^2$)
N_i	Occupation number in Ref. ε_i level
N_o	Average occupation number of receptor sites N_m
n_i	Number of particles
p	Nitrogen equilibrium pressure (mmHg)
p^0	Nitrogen saturation pressure (mmHg)
PDI	Polydispersity index
Q_a/V_{N_2}	Amount adsorbed/Volume adsorbed ($cm^3 STP.g^{-1}$)
Q_{a-M}	Amount adsorbed for a monolayer model ($cm^3 STP.g^{-1}$)
Q_{a-MBET}	Amount adsorbed for a BET model ($cm^3 STP.g^{-1}$)
Q_m^{sat}	Saturated amount adsorbed at the monolayer ($cm^3 STP.g^{-1}$)
Q_{BET}^{sat}	Saturated amount adsorbed at the monolayer predicted by the BET model ($cm^3 STP.g^{-1}$)
Q_{calc}	Theoretical amount adsorbed ($cm^3 STP.g^{-1}$)
Q_{meas}	Experimentally determined amount adsorbed ($cm^3 STP.g^{-1}$)
R	Universal gas constant ($8.3143.10^{18}$ $J.nm^2(K.mol.m^2)^{-1}$)
r_p	Pore radius (nm)
r_K	Kelvin radius (nm)
S_{BET}	BET specific surface area (m^2/g)
S_{tot}	Total surface area (m^2/g)
S_{Cal}	Geometrical surface area (m^2/g)
T	Temperature (K)
t	Statistical film thickness (nm)
V	Volume occupied by a molecule (cm^3)
V_T	Total pore volume (cm^3/g)
V_L	Nitrogen molar volume (34.68 cm^3/mol)
$V_{\mu p}$	Micropore volume (cm^3/g)
w	Pore width (nm)
w_0	Average pore width (nm)
w_{min}	Minimum pore width (nm)
w_{max}	Maximum pore width (nm)
Z_{gtr}	Partition function of translation
z_{gc}	Grand canonical partition function for a single receptor site
z_{gtr}	Partition function of translation per unit volume
μ	Chemical potential of a molecule (kJ)
ε	Adsorption site energy(kJ/mol)
ε_i	Adsorption energy of the receptor site$i$ (kJ)
ε_L	Heat of liquefaction as assumed by BET model (kJ/mol)
γ	Surface tension of the liquid adsorbate (8.88×10^{-3} N/m)
α	Constant
σ	Dispersion of the Gaussian distribution (kJ/mol)
$-\Delta E^v$	Vaporization energy (kJ/mol)

conducted studies on pore size distribution (PSD) by applying the Kelvin equation [6,14], which is considered valid for the capillary condensation theory and it is used in various macroscopic methods to evaluate the mesoporous region. Among these macroscopic methods are: Barrett, Joyner and Halenda (BJH) [15], Pierce [16], Dollimore and Heal (DH) [17], BJH modified by Kruk, Jaroniec and Sayari (BJH-KJS) [18] and others. A macroscopic method to improve the BJH and DH methods, which takes into account the correct filling/emptying mechanism of each type of pores, denominated as VBS method (Villarroel-Barrera-Sapag) was proposed also to evaluate PSD of mesoporous materials. This last method adds a correction term, f_c, to the original Kelvin equation (r_K), in order to avoid the underestimation given by the r_K itself (obtained by unmodified/original Kelvin equation) [19,20].

Among phenomena that may be involved in physical adsorption can be considered: monolayer adsorption, multilayer adsorption and condensation in pores (larger than micropores). As a result, the interpretation of adsorption studies can be complicated and many attempts have been conducted to looking for model expressions that can describe in the best way the associated physical adsorption phenomenon. In this sense, many authors proposed empirical models that describe different type of isotherms [21,22]. However, most of these models contain constants that do not give any supplementary information for describing the adsorption process. Furthermore, in some cases the expressions (or equations) of these constants found in the bibliography have no physical significance or relationship with the physicochemical parameters intervening in the adsorption process. The theoretical modeling of adsorption isotherms is crucial to the design and scale-up of practical adsorption processes. In our previous works, it was demonstrated that statistical physics approach is a powerful way to analytically establish models that are thermodynamically consistent and the physicochemical parameters intervening in the adsorption process are taken into account in the theoretical treatment [23–28]. They overcome the drawbacks in the ad hoc expressions that did not contain the physical realities.

The present work is an attempt to propose a new method for the evaluation of PSD based on statistical mechanics approach and on a segmentation procedure for polystyrene (PS) latex along with its copolymers such as Poly (styrene-co-hydroxyethyl methacrylate acid) (PS-HEMA), Poly(styrene-co-acrylic acid) (PS-AA), Poly(-styrene-co−methacrylic acid) (PS-MAA) and Poly (styrene-co−itaconic acid) (PS-IA). The goal of this method is to develop two theoretical models based on statistical mechanics approach to take into account of the monolayer adsorption as well as the condensation/evaporation phenomena. The formation of complete monolayer was obtained up to relative pressure (i.e., absolute pressure and saturation pressure ratio) value of 0.35. Then, the number of adsorbed layers goes to the infinity [26] and considers appropriate mechanisms of capillary condensation and evaporation in the meso and macropores when the relative pressures are higher than 0.35 [29]. The aim of this new proposed method is to fit the nitrogen adsorption/desorption experimental data by segmentation procedure using a *monolayer* and a *modified BET* models [26,28], as local isotherms, for the first and second regions, respectively. These two local isotherms are combined with a

Gaussian distribution function and the PSD can be obtained. The idea of segmentation is a good tool to take into account the physical phenomenon occurred in each relative pressure region. The main goal of this study is to present a reliable theoretical approach for evaluation of PSD for mesopores and macropores polymer latices from nitrogen adsorption-desorption isotherms. The work is focused on the comparison of the presented approach with three well known previous methods such as BJH, VBS and the NLDFT model, pointing out the differences among them in order to determine the most suitable method.

2. Experimental

2.1. Materials

Reference material Styrene (S) was purchased from Sigma-Aldrich, 99%, and purified with a 0.1 M sodium hydroxide solution to remove inhibitor. Acrylic acid (AA), 99%, itaconic acid (IA), 99%, methacrylic acid (MAA), 99%, and hydroxyethyl methacrylate (HEMA), 97%, and potassium persulfate (KPS), 99%, were purchased from Sigma-Aldrich and used as received without purification. Distilled water was used in all the synthesis.

2.2. Synthesis of latex particles

The synthesis procedure for spherical particles of different kinds of latex was described elsewhere [30–32]. Polystyrene (PS) was prepared by polymerization of styrene, and hydroxyethyl methacrylate, acrylic acid, methacrylic acid and itaconic acid was used as copolymer to obtain poly[styrene-co-hydroxyethyl methacrylate], PS-HEMA, poly[styrene-co-acrylic acid], PS-AA, poly[styrene-co-methacrylic acid], PS-MAA and poly[styrene-co-itaconic acid], PS-IA.

2.3. Characterization methods

Field emission scanning electron microscopy (FESEM) was carried out in a JEOL-6335F microscope at 12 μA and 5 kV, and before observation the samples were coated with a gold film. The number-average diameter of the particles, D_n, was estimated from the micrographs of each sample, and the polydispersity index, *PDI*, was calculated using D_n and the mass average diameter, D_m [30,33,34]. From the mean particle size (D_n), the geometrical surface area, S_{Cal}, was calculated for each sample.

The N_2 adsorption/desorption isotherms at 77 K were measured using a manometric instrument Micromeritics ASAP 2020. All samples were outgassed at 50 °C for 6 h previous to nitrogen adsorption/desorption analysis. Textural properties of the functionalized polystyrene latices under study were determined from nitrogen adsorption-desorption isotherms data. The specific surface area (S_{BET}) of the samples was estimated with the Brunauer, Emmet and Teller (BET) method [35] using the linear part ($0.05 < p/p^0 < 0.25$) [19,36] (where p and p^0 denote the equilibrium and saturation pressures of nitrogen, respectively) of the adsorption isotherm and assuming a closely packed BET monolayer, using the value of 0.162 nm^2 as the molecular cross-sectional area for adsorbed nitrogen [7,29]. The total pore volume (V_T) was obtained by Gurvich's rule [29] at a relative pressure of 0.99. The α_s-plot method [6,37] was used to calculate the micropore volume ($V_{\mu p}$) and total surface area (S_{tot}) using the LiChrospher Si-1000 macroporous silica gel as the reference adsorbent [38].

3. PSD determination methods

Finding a reliable, accurate, and flexible method for PSD determination of porous adsorbents still remains an important concern in the area of characterization of porous materials. Although a large number of studies have been done in this area, some constraints such as type of adsorbate, adsorbent characteristics, adsorption temperature, applicable range of pore size, and range of relative pressure limit the applicability of each model in all cases [39]. The absence of such method is tangible by rapid development of new porous materials and their wide applications in various areas.

3.1. Previous methods

3.1.1. BJH method

The most often used method to determine the PSD in mesoporous materials was introduced by Barrett, Joyner and Halenda (BJH) [15], based on the capillary condensation theory, using the Kelvin equation, where a cylindrical pore geometry is assumed and the desorption branch isotherm data are used. This model is corrected for multilayer adsorption using statistical film thickness [15].

Pore radius, r_p, is the sum of Kelvin radius, r_K, and the statistical film thickness, t [18]:

$$r_p = r_K + t \tag{1}$$

where, r_K is calculated from Kelvin equation for hemispherical menisci:

$$r_K = \frac{-2 \cdot \gamma \cdot V_L}{RTln\left(\frac{p}{p^0}\right)} \tag{2}$$

where γ is the surface tension of the liquid adsorbate, V_L is its molar volume, R is the universal gas constant, $8.3143 \cdot 10^{18}$ $J.nm^2(K.mol.m^2)^{-1}$, and T is the absolute temperature. For nitrogen at 77 K (γ=8.88×10^{-3} N/m, $V_L = 34.68$ cm^3/mol) [40], the Kelvin equation is reduced to the following expression where r_K is in Ref. *nm* [15].

$$r_K = \frac{-0.414}{log\left(\frac{p}{p^0}\right)} \tag{3}$$

The obtained film thickness curve $t(p/p^0)$ can be accurately represented in the relative pressure range from 0.1 to 0.95 by the Harkins-Jura/Kruk-Jaroniec-Sayari (HK-KJS) equation of the following form [18,41]:

$$t\left(\frac{p}{p^0}\right) = 0.1\left[\frac{60.65}{0.03071 - log\left(\frac{p}{p^0}\right)}\right]^{0.3968} \tag{4}$$

However, it was found that this macroscopic method overestimates the capillary condensation/evaporation pressure and subsequently the pore size is underestimated (up to 25% for mesoporous materials consisting of pores $\leq$10 *nm*) [18,42]. Regarding this fact, an improvement of BJH method has been reported by Villarroel-Barrera-Sapag (VBS method) [19,20].

3.1.2. VBS method

VBS method (Villarroel-Barrera-Sapag), is an improvement method in comparison with BJH one. It is developed based on silica ordered mesoporous materials with cylindrical and spherical pore geometries [19,20]. In the BJH method the pore radius (r_p) is calculated by the sum of the Kelvin radius (r_K) and the statistical film thickness of adsorbed nitrogen (t). VBS method modifies the original Kelvin equation with the addition of a correction term, f_c,

which is selected using a self-consistent criterion (i.e. the reconstructed isotherm should fit the original one).

Therefore, the Kelvin radius (r_K) (in nm) for cylindrical (adsorption branch) or hemispherical (desorption branch) meniscus, is modified by the addition of a correction term (f_c) as it is shown in Eqs. (5) and (6), respectively.

$$r_K = -\frac{0.48103}{ln\left(\frac{p}{p^0}\right)} + f_c \tag{5}$$

$$r_K = -\frac{0.96207}{ln\left(\frac{p}{p^0}\right)} + f_c \tag{6}$$

In the material under study the VBS method was applied in the relative pressure range from 0.05 to 0.99 using the desorption branch data.

3.1.3. NLDFT model

The NLDFT model has been developed to evaluate the pore size distribution of microporous and mesoporous materials [43]. In this work, the NLDFT method was applied using the ASiQwin software, v.2.0 (Quantachrome Instruments), where the kernel selected for cylindrical pore geometry was N_2 at 77 K on silica, using the desorption branch.

3.2. New proposed method

For nitrogen adsorption isotherms of some materials, the monolayer is usually completed up to relative pressures close to 0.35, and at higher values the number of adsorbed layers could go to infinity. This behavior is appropriate for materials with large mesopores or macropores that present isotherms type II or III according to the IUPAC classification [44] where the amount adsorbed quickly increases at high relative pressures close to 1. The new proposed method arising out of BET model but considering the capillary phenomenon with appropriate mechanisms of condensation and evaporation in the large mesopores or macropores [26]. Regarding this fact, we proposed to fit experimental isotherm data by a segmentation procedure. For the first and second regions, a monolayer and a modified BET models were used as local isotherms [26], respectively. The two local isotherms were coupled to a Gaussian distribution function to fit the experimental data. Then a statistical physics approach [21] is used to establish the analytical expressions for two models as described in previous works [26,45].

To perform calculation, we assumed some simplified hypotheses. We consider that a variable number of molecules per unit of volume N, are adsorbed onto N_M receptor sites per unit of mass adsorbent. Furthermore, it is assumed that any given receptor site can be empty or occupied according to the state of occupation number N_i, with an adsorption energy ε and a chemical potential μ.

Moreover, the adsorption process should include a stoichiometric coefficient n, such that:

$$n\mathcal{M} + S \leftrightarrows \mathcal{M}_n S \tag{7}$$

Where n is a stoichiometric coefficient representing the fraction or the number of molecule(s) $\mathcal{M}$ adsorbed per site S.

It is necessary to make some assumptions as the bases of an initial postulate. As a first approximation, the adsorbate molecules are treated as an ideal gas [22,26], i.e., the lateral interactions are neglected. Adsorption involves an exchange of particles from the free state to the adsorbed one, so the use of Grand Canonical ensemble is mandatory to take into account of particle number variation through the introduction of a variable chemical potential. We take into account also only of the translation degrees of freedom.

Thus, to treat the adsorption phenomenon by using statistical physics approach, the departure point is the Grand Canonical partition function for a single receptor site, z_{gc} [26], which is written as follows:

$$z_{gc} = \sum_{N_i} e^{-\beta N_i(\varepsilon_i - \mu)} \tag{8}$$

where $(\varepsilon_i)\,(kJ)$ is the adsorption energy of the receptor site i, $\mu\,(kJ)$ is the chemical potential, N_i is the occupation number and β is defined as being $(1/k_BT)$, where k_B is the Boltzmann's constant.

The total Grand Canonical partition function related to N_m identical and independent receptor sites per surface unit is equal to $(z_{gc})^{N_m}$.

The occupation number for N_m identical receptor sites is given by the following equation [26,28]:

$$N_o = k_BT\,\frac{\partial \ln(z_{gc})^{N_m}}{\partial \mu} \tag{9}$$

Then, according to the Equation (7), the total number of adsorbed molecules is given as:

$$Q_a = nN_o \tag{10}$$

The fugacity expression can be used to relate the chemical potential and the pressure as follows [26]:

$$e^{\beta\mu} = \frac{N}{Z_{gtr}} = \beta\frac{p}{z_{gtr}} \tag{11}$$

N is the number of adsorbate molecules, p (mmHg) is the pressure of adsorbed molecules at equilibrium, $\mu\,(kJ)$ is the chemical potential of a molecule assimilated for an ideal gas, z_{gtr} is the partition function of translation per unit volumeand Z_{gtr} is the partition function of translation that can be written as follows [26]:

$$Z_{gtr} = V\left(\frac{2\pi m k_B T}{h^2}\right)^{3/2} \tag{12}$$

where $m\,(g)$ is the mass of an adsorbed molecule, $V(cm^3)$ is the volume occupied by a molecule, $h\,(6.626\times10^{-34}\,m^2kg/s)$ is Planck's constant and k_B $(1.380\times10^{-23}\ m^2kg/s.K)$ is the Boltzmann's constant.

This partition function of translation can be expressed according to the saturated vapor pressure as follows [26]:

$$Z_{gtr} = \beta p^0 e^{\frac{-\Delta E^v}{RT}} \tag{13}$$

where $-\Delta E^v\ (kJ/mol)$ is the vaporization energy, p^0(mmHg) is the saturated vapor pressure, R $(8.314\ J/K\ mol)$ is the universal gas constant and T (K) is the absolute temperature.

By using the fundamentals of thermodynamic equilibrium, the mass action law is written according to Equation (7):

$$\mu_m = \frac{\mu}{n} \text{and}\ \ \varepsilon_m = \frac{\varepsilon}{n} \tag{14}$$

where the index m is related to the adsorbed molecule.

For a monolayer model adsorption, the receptor site can be empty ($N_i = 0$) or occupied once ($N_i = 1$). Then, the partition function of one receptor site is written as:

$$z_{gc} = 1 + e^{\beta(\varepsilon_1 + \mu)} \tag{15}$$

This leads to the following expression of the amount adsorbed, Q_{a-M}:

$$Q_{a-M}\left(\frac{p}{p^0}\right) = \frac{Q_m^{sat}}{1 + e^{\frac{\varepsilon}{RT}}\left(\frac{p^0}{p}\right)^n} \tag{16}$$

with p/p^0 as relative pressure and Q_m^{sat} as saturated amount adsorbed at the monolayer.

If the adsorption occurs with a capillary condensation, the receptor site can be empty ($N_i = 0$), occupied once ($N_i = 1$), twice ($N_i = 2$), or infinity ($N_i = \infty$). In such case, the Grand Canonical partition function is written as:

$$z_{gc} = \sum_{N_i=0}^{\infty} e^{-\beta N_i(\varepsilon_i - \mu)} \tag{17}$$

Accordingly, the amount adsorbed, Q_{a-MBET}, is given by the following expression:

$$Q_{a-MBET}\left(\frac{p}{p^0}\right) = Q_{BET}^{sat}\frac{e^{-\varepsilon/RT}\left(\alpha\cdot\frac{p}{p^0}\right)^n}{\left[1-\left(\frac{p}{p^0}\right)^n + e^{-\varepsilon/RT}\left(\alpha\cdot\frac{p}{p^0}\right)^n\right]\left[1-\left(\frac{p}{p^0}\right)^n\right]} \tag{18}$$

with α as constant, ($\alpha = e^{\varepsilon_L^{/RT}}$) such as ε_L is that for the second and higher layers and is equal to the liquefaction heat as assumed by BET model [35] and Q_{BET}^{sat} as saturated amount adsorbed at the monolayer predicted by the BET model.

According the bibliography [29,46], an empirical dependence between the adsorption energy, ε, and the pore width can be expressed as:

$$\varepsilon = \frac{\mathscr{K}}{w} \tag{19}$$

where $\mathscr{K}$(kJ.nm/mol) is the characteristic constant for a defined adsorbate/adsorbent system and w (nm) is the pore width.

Equations (16), (18) and (19) have been extended for predicting the pore size distribution by assuming a PSD function $f(w)$,.The most commonly used form of adsorption energy distribution is a Gaussian function. This leads us to write the pore size distribution, $f(w)$, as follows:

$$f(w) = \frac{\mathscr{K}}{w^2\sigma\sqrt{2\pi}}exp\left(-\frac{(1/w - 1/w_0)^2.\mathscr{K}^2}{2\sigma^2}\right) \tag{20}$$

where w_0 is the average pore width and σ is the dispersion of the Gaussian distribution.

Finally, the integral equations which use the monolayer model in the first region and the modified BET model in the second region as local isotherms to fit our experimental data can be written as follows in Equations (21) and (22), respectively:

$$Q_{a-GM}\left(\frac{p}{p^0}\right) = \frac{\mathscr{K}Q_m^{sat}}{\sigma\sqrt{2\pi}}\int_{w_{min}}^{w_{max}}\frac{1}{w^2\left[1+e^{\mathscr{K}/wRT}\left(\frac{p^0}{p}\right)^n\right]}exp\left(-\frac{(1/w - 1/w_0)^2.\mathscr{K}^2}{2\sigma^2}\right)dw \tag{21}$$

$$Q_{a-GMBET}\left(\frac{p}{p^0}\right) = \frac{\mathscr{K}Q_{BET}^{sat}\left(\alpha\cdot\frac{p}{p^0}\right)^n}{\sigma\sqrt{2\pi}\left[1-\left(\frac{p}{p^0}\right)^n\right]}\int_{w_{min}}^{w_{max}}\frac{e^{-\mathscr{K}/wRT}}{w^2\left[1-\left(\frac{p}{p^0}\right)^n + e^{-\mathscr{K}/wRT}\left(\alpha\cdot\frac{p}{p^0}\right)^n\right]}exp\left(-\frac{(1/w - 1/w_0)^2\cdot\mathscr{K}^2}{2\sigma^2}\right)dw \tag{22}$$

where w_{min} and w_{max} are the minimum and the maximum pore width, respectively.

The adsorption equilibrium data in each segment, i.e., up to 0.35 for the first segment and between 0.35 and 0.99 for the second segment, were fitted independently with GM and GMBET models, respectively, by minimizing the sum of the squares of the errors (ERRSQ) [47]:

$$ERRSQ = \sum_{i=1}^{j}(Q_{calc} - Q_{meas})_i^2 \tag{23}$$

Where Q_{calc} isthetheoretical amount adsorbed, which has been calculated with the local isotherm models, Q_{meas} is the experimentally determined amount adsorbed and j is the number of data points.

The corresponding absolute relative error (ARE) values were estimated from equation (24) [48] and the optimum fitting parameters, namely, n, Q_m^{sat}, Q_{BET}^{sat}, w_{min}, w_{max}, w_0, α, σ, and $\mathscr{K}$ were obtained.

$$ARE\ (\%) = \frac{100}{j}\sum_{i=1}^{j}\left|\frac{Q_{calc} - Q_{meas}}{Q_{meas}}\right|_i \tag{24}$$

Then, the PSD are obtained by fitting procedure and the calculation method was based on the solver add-in with Microsoft's spreadsheet, Excel (Microsoft Corporation, 2007). We are based on the Generalized Reduced Gradient algorithm with nonlinear optimization.

4. Results and discussion

4.1. FESEM micrographs

Fig. 1 shows FESEM micrographs of PS-HEMA, PS-AA, PS-MAA, PS and PS-IA particles. This particles are spherical with mono-

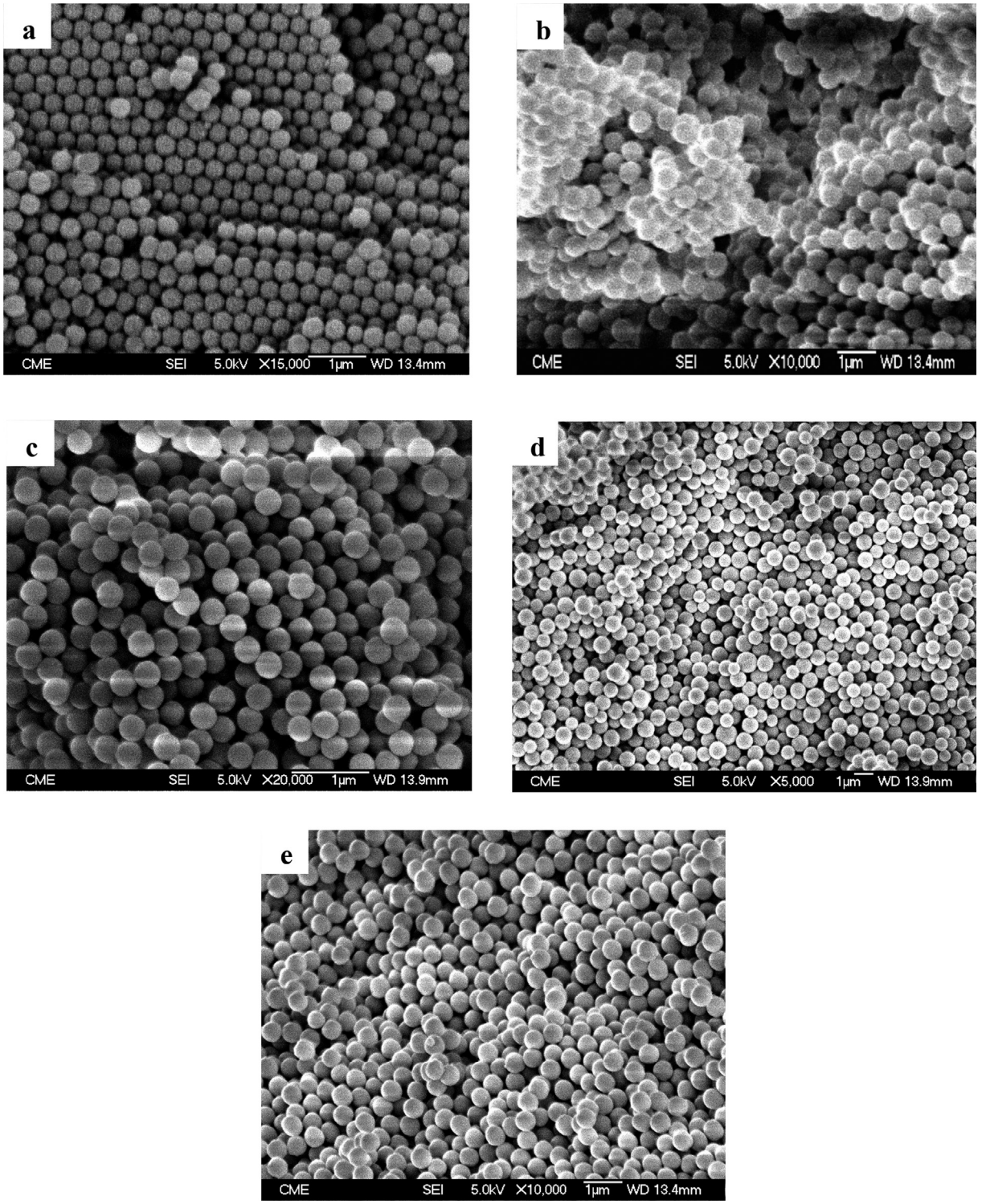

Fig. 1. SEM micrographs of particles under study: PS-HEMA (a), PS-AA (b), PS-MAA (c), PS (d), PS-IA (e).

sizes diameter [34]. The number-average diameter, $D_n = \frac{\sum n_i D_i}{\sum n_i}$, of particles and the polydispersity index (PDI = D_m/D_n) of particles were calculated using SEM data from Ref. D_n and mass average diameters, $D_m = \frac{\sum n_i D_i^4}{\sum n_i D_i^3}$, where n_i is the number of particles with diameter D_i [30,33,34]. The number of particle diameter increases from 339 nm (PDI = 1.002) to 653 nm (PDI = 1.007) (Table 1). The

Table 1
Textural properties of the latex particles.

Material	PS-HEMA	PS-AA	PS-MAA	PS	PS-IA
D_n (nm)	342	404	339	653	508
PDI	1.003	1.005	1.002	1.007	1.004
$S_{BET}(m^2/g)$	17.0	15.1	18.6	9.0	12.6
$S_{Cal}(m^2/g)$	16.7	14.1	16.9	8.8	11.3
$V_T(cm^3/g)$	0.16	0.08	0.12	0.03	0.08
$V_{\mu p}(cm^3/g)$	0	0	0	0	0
$S_{tot}(m^2/g)$	20	16	21	9	13

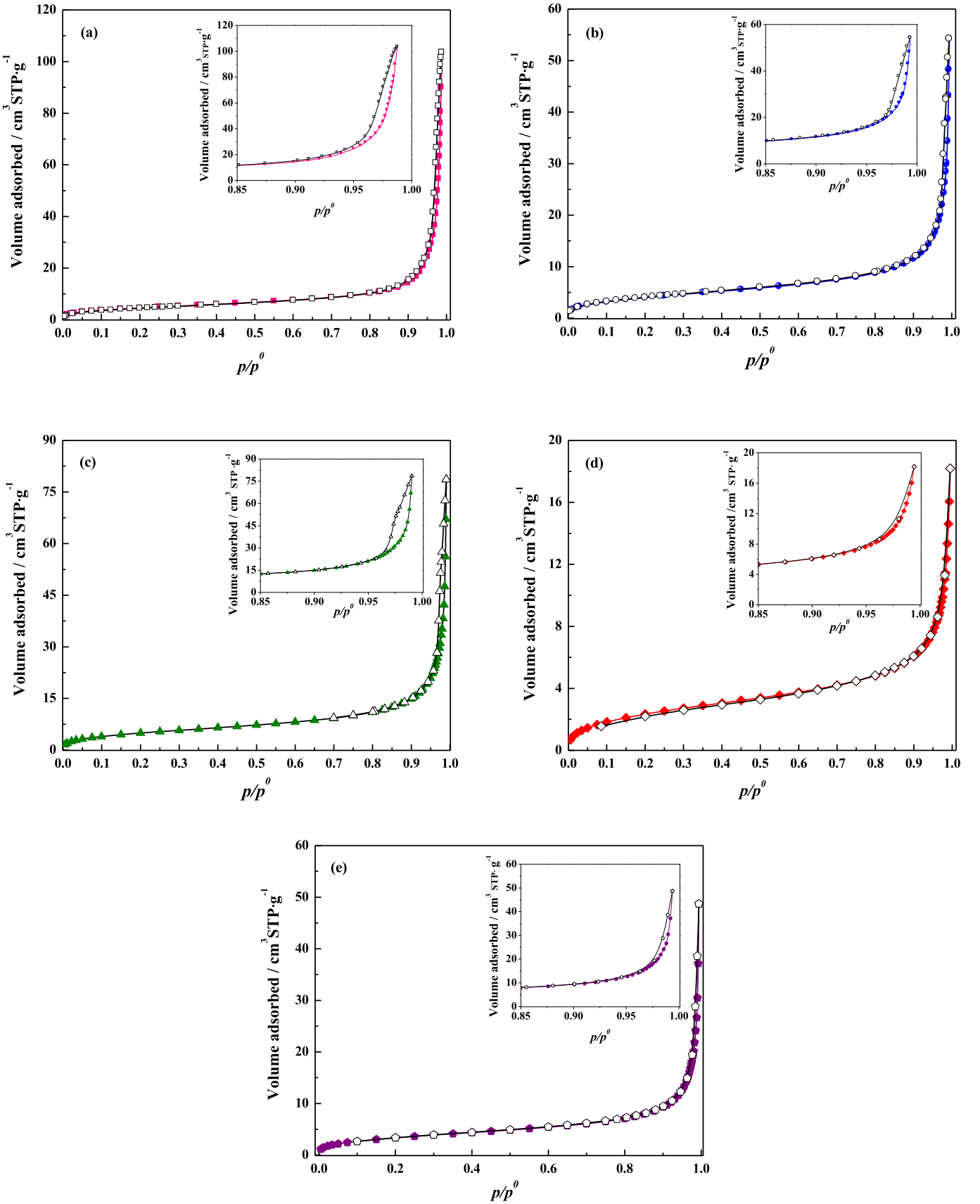

Fig. 2. Nitrogen adsorption–desorption isotherms at 77 K for the different latex: PS-HEMA (a), PS-AA (b), PS-MAA (c), PS (d), and PS-IA (e) (filled symbol: adsorption; empty symbol: desorption).

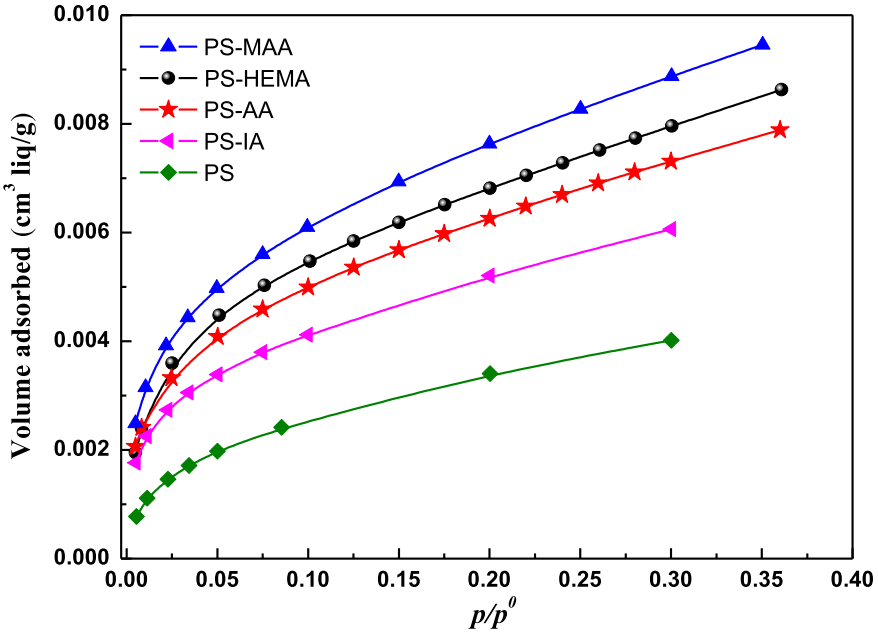

Fig. 3. Volume adsorbed (as liquid) in the monolayer region for the different latex.

difference between the diameters of the PS particle and its copolymer is most probably due to the steric hindrance brought by chemical structure and the percentage of the used comonomer [34].

From the mean particle size (D_n), the geometrical surface area, S_{Cal}, was calculated for each sample (Table 1) and the results were compared with the specific surface area obtained from nitrogen adsorption isotherm data, S_{BET}.

4.2. Nitrogen adsorption-desorption analyses

4.2.1. Experimental isotherms and textural properties

Fig. 2 shows the N_2 adsorption-desorption isotherms measured at 77 K on the latex particles. In all cases, the isotherms are type II or III (typical of materials with a weak adsorbent–adsorbate interaction) with hysteresis loops type H3 (typical of solids with aggregates or agglomerates of particles) [44]. All samples showed an abrupt increase at relative pressures higher than 0.9, which is due to the presence of large mesopores and/or macropores [41].

Fig. 3 shows the nitrogen volume adsorbed (as liquid) in the monolayer region, where it can be seen that this volume adsorbed is inversely dependent on the particle size. Furthermore, the specific surface area depends on other factors such as the breadth of the particle size distribution [49]. For broad particle size distribution (polydisperse) the specific surface area is higher than that ones with narrow particle size distribution (monodisperse). Fig. 4 illustrates the concept of monodisperse and polydisperse particles. This figure also shows, in a polydisperse latex, that the addition of small grains within the pores placed between the larger ones can reduce the porosity. Table 1 shows the PDI values, where it can be seen that the polystyrene (PS sample) is the most polydisperse sample, and then it has the low monolayer amount adsorbed as mentioned previously which shows a low porosity (Fig. 7).

Table 1 also shows textural properties determined from nitrogen adsorption-desorption isotherms data at 77 K of functionalized polystyrene latices under study. Fig. 5 shows the α_s-plot curve for the PS-HEMA evidencing the absence of micropores, and same behavior was obtained for the other samples. From the slope of the linear region of the α_s-plot curve, external surface area of these five samples is obtained. In this case, the external surface area is the total surface area (S_{tot}) due to there are not micropores. After this linear region, a quick increase in the volume adsorbed is observed at higher α_s values due to the capillary condensation of nitrogen in the mesopores [50]. Table 1also shows the geometrical surface area

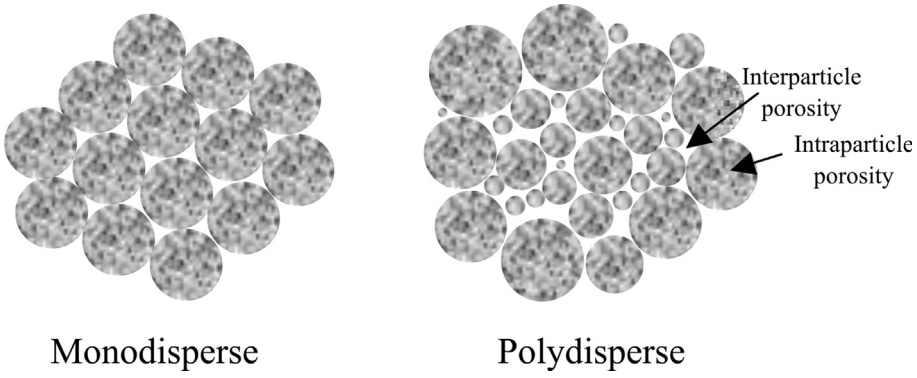

Fig. 4. Dense packing of monodisperse and polydisperse spheres.

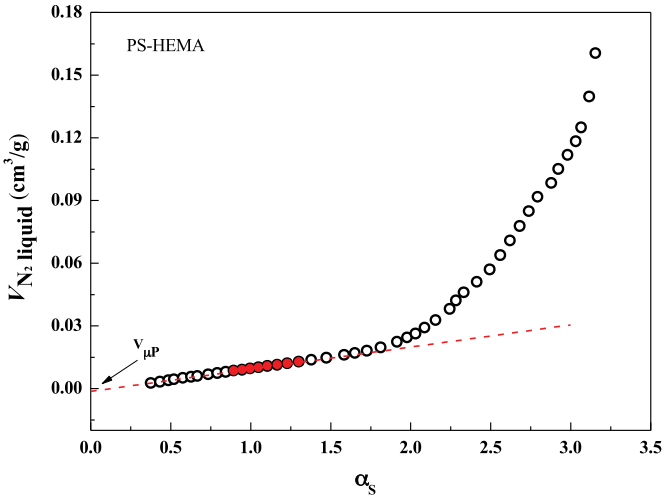

Fig. 5. α_s-plot curve of the PS-HEMA sample. Filled symbols represent the selected range of α_s values.

(S_{Cal}) which is similar to S_{BET} and S_{tot} values corroborating the above mentioned. Polystyrene presents a lower specific surface area value(9.0 m^2/g), mean while for the copolymers this value increases till 18.6 m^2/g and due to the percentage of the comonomers used, thus generating particles of different sizes.

4.2.2. Pore size distribution (PSD)

In the PSD studies, the selection of suitable branch has been subject of several discussions by other authors, justifying the use of adsorption or desorption branches [18,51]. The selection of the desorption branch is the most accepted, when both branches can be selected, because it reflects transitions near the equilibrium phase [19]. The use of the desorption branch should be carefully analyzed, when the hysteresis loop for nitrogen isotherms at 77 K closing near to 0.40–0.45, in relative pressure (cavitation phenomenon). In these cases, the better chosen branch is the adsorption one [19].

For all samples (Fig. 2), the hysteresis loops close near 0.90–0.95 of relative pressure and, hence the cavitation phenomenon is absent. For these specific samples, both branches can be selected.

The PSDs of five samples have been determined using the new proposed method (GM-GMBET). Fig. 6 reports the experimental nitrogen desorption isotherm for PS-HEMA, along with the fitted isotherm using the segmentation procedure, i.e., Gauss monolayer for the lower relative pressure (up to 0.35) and Gauss modified BET for the higher relative pressure (>0.35). The PSD that was obtained for this example (PS-HEMA) from the fitting procedure is shown in the same figure (Fig. 6). Good fit to the experimental isotherm is observed for PS-HEMA sample with only small deviations at high relative pressure and same behavior was found for the other ones. Adjustment parameters of all the samples for both branches, adsorption and desorption, are shown in Table 2.

The PSD obtained for all samples from the desorption branch data are shown in Fig. 7 where it was found that the polymer latex are mainly mesoporous and macroporous, with only a small mesopores volume with pore sizes around 10 nm. The small contribution of mesopores obtained by the new developed method can be attributed to the intraparticle porosity (Fig. 4).

According Table 2, the values of ARE are small for all studied samples except for PS latice when the proposed method is applied at $p/p^0 > 0.35$. This fact is due to that this sample does not present meaningful porosity and then any peak in the PSD (Figs. 7 and 8(d)). For the other samples, the minimum pore width values, w_{min}, for the desorption and adsorption branches are between 0.001 nm and 1.68 nm taking of account in all the relative pressure range (Table 2). This value range is expected due to w_{min} value should be less than the minimum pore size for the PSD obtained with the proposed method (i.e. 2 nm). The upper limit of the PSD is determined by the width of larger mesopores and also macropores which condenses at the highest experimental pressure. The maximum pore width, w_{max}, is set to larger mesopores and/or macropores. When the new proposed method is applied at $p/$

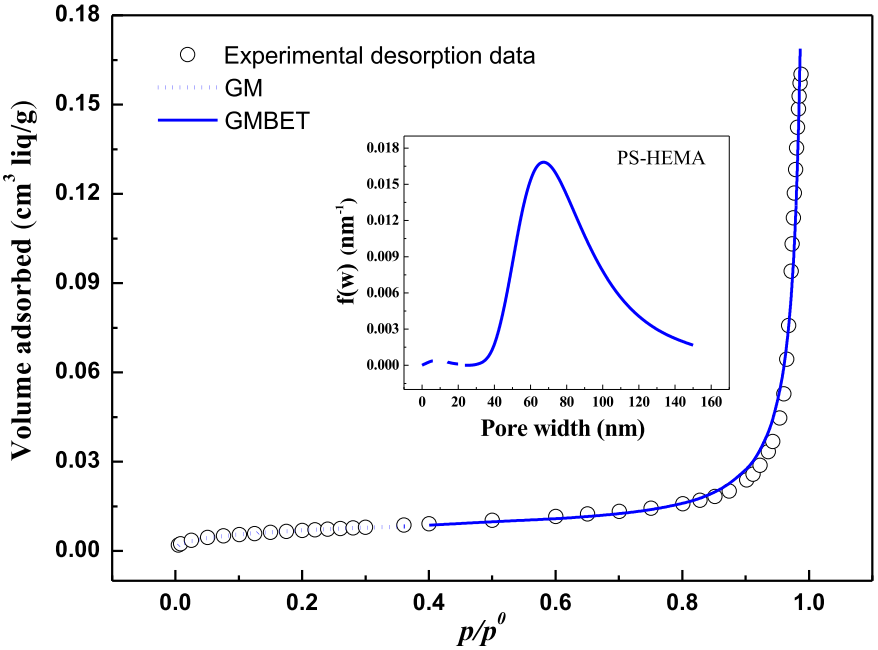

Fig. 6. Desorption isotherms (experimental and theoretical) and pore size distribution for PS-HEMA sample. The circles are the experimental data; the solid and broken lines are the fitted isotherms with GM and GMBET models, respectively.

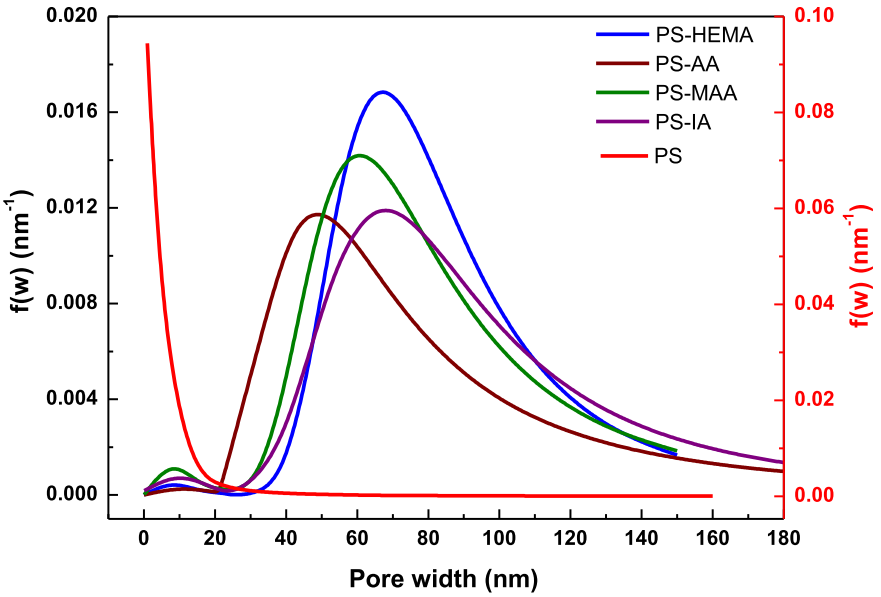

Fig. 7. Pore size distribution from desorption branch using the new proposed method.

$p^0 \leq 0.35$ then; value is lower than 1 which means indicating that the monolayer is not complete. At $p/p^0 > 0.35$, the n value is higher than 1 due to the multimolecular adsorption occurs because the capillary condensation/evaporation on meso-macropores. The difference between the obtained PSD (Fig. 7) in the macropores range is attributed to particle size of the copolymer samples.

For all the materials under study the PSDs obtained by the new proposed method (GM/GMBET) were compared with the microscopic method NLDFT and macroscopic methods such as BJH and VBS. This comparison was carried out in order to find the main differences between them taking into account all of them have been development under different physical theories. In the

Table 2
Fitting parameters obtained by using the proposed method for both adsorption and desorption branches.

	p/p^0 segment	Parameter	PS-HEMA	PS-AA	PS-MAA	PS	PS-IA
Adsorption branch	$0<p/p^0 \leq 0.35$	n	0.418	0.413	0.383	0.419	0.379
		$Q_m^{sat}(cm^3STP.g^{-1})$	0.100	0.130	0.335	0.162	0.22658
		$w_{min}(nm)$	0.090	0.033	0.026	0.993	0.046
		$w_{max}(nm)$	249	250	150	150	180
		$\sigma(kJ/mol)$	0.096	4.01	55	50	50
		$\mathscr{K}$(kJ.nm/mol)	0.068	1.99	12	12	12
		$w_0(nm)$	30	30	29.999	30	30
		ARE (%)	2.814	3.639	2.739	2.233	3.161
	$p/p^0 > 0.35$	n	5.139	33.592	20.469	13	30.452
		$Q_{BET}^{sat}(cm^3STP.g^{-1})$	0.009	0.031	0.027	0.028	0.017
		$w_{min}(nm)$	0.045	0.370	1.68	5.00	0.159
		$w_{max}(nm)$	150	222	250	150	250
		$\sigma(kJ/mol)$	0.030	13.5	6.77	8.97	14
		α	5.075	3.914	4.931	4	8.660
		$\mathscr{K}$(kJ.nm/mol)	12	1200	1200	18.7	2500
		$w_0(nm)$	79.998	118.672	117.954	50	90.008
		ARE (%)	7.076	9.714	8.037	31.261	8.853
Desorption branch	$0<p/p^0 \leq 0.35$	n	0.441	0.428	0.383	0.467	0.373
		$Q_m^{sat}(cm^3STP.g^{-1})$	0.477	0.551	0.305	0.161	0.230
		$w_{min}(nm)$	0.009	0.002	0.044	0.993	0.048
		$w_{max}(nm)$	150.001	199.998	150	150	190.002
		$\sigma(kJ/mol)$	11.997	11.971	49.998	50.003	50.007
		$\mathscr{K}$(kJ.nm/mol)	1.098	1.131	12.004	11.995	11.969
		$w_0(nm)$	30	30	33	30	33
		ARE (%)	2.866	3.998	2.731	1.495	3.213
	$p/p^0 > 0.35$	n	4.326	20.285	13.008	13	30.805
		$Q_{BET}^{sat}(cm^3STP.g^{-1})$	0.013	0.020	0.026	0.026	0.030
		$w_{min}(nm)$	0.02	0.383	0.001	5	0.048
		$w_{max}(nm)$	150.013	200.066	150.008	160	250.026
		$\sigma(kJ/mol)$	0.053	4.347	2.971	8	14.005
		α	4	3.732	5.439	4	8.036
		$\mathscr{K}$(kJ.nm/mol)	12	449.966	499.998	20	2500
		$w_0(nm)$	80	80.027	79.993	120	89.997
		ARE (%)	9.869	12.055	10.383	26.595	8.624

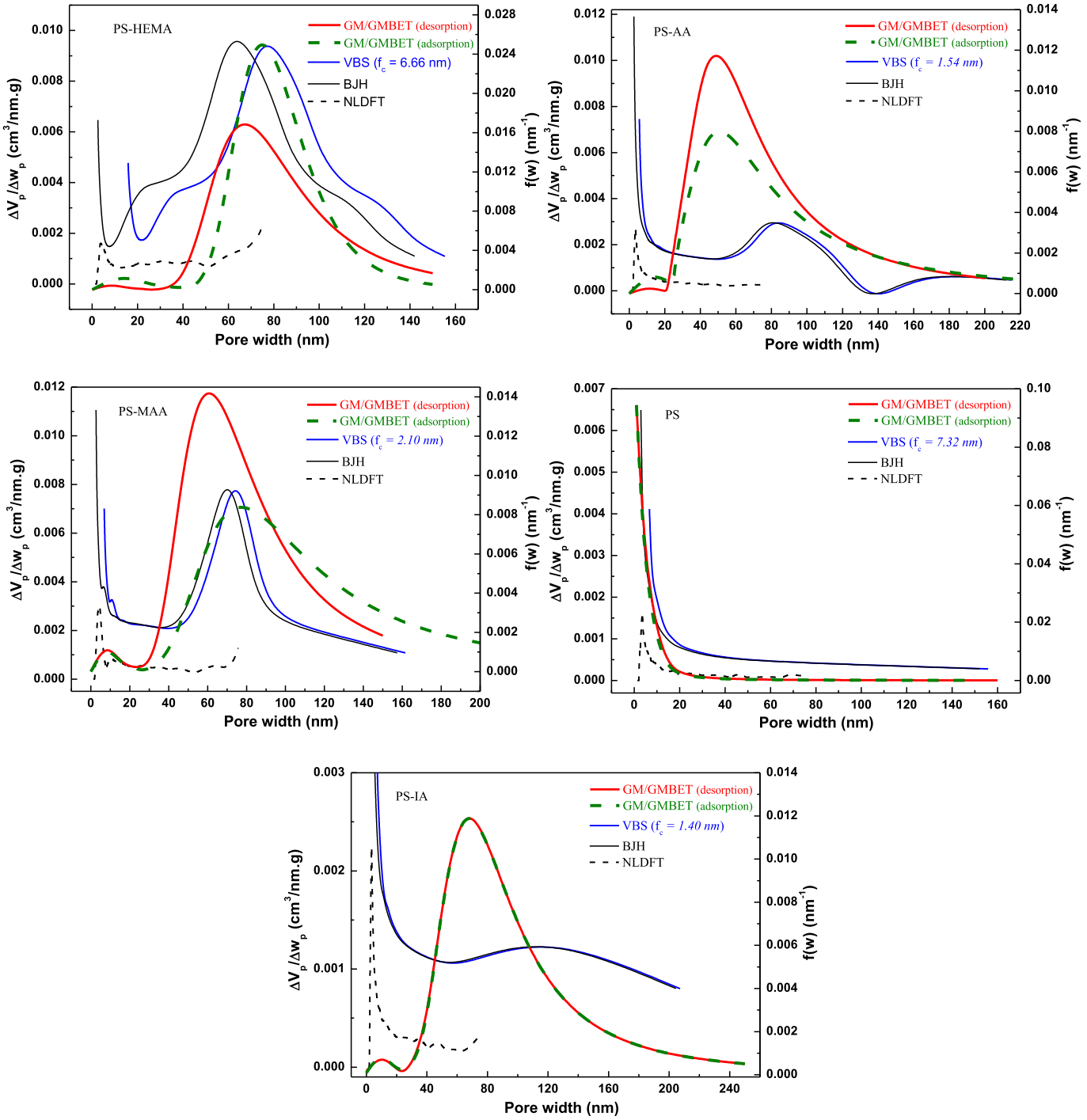

Fig. 8. Comparison of the PSD for all samples obtained by BJH, VBS and NLDFT methods and by the new proposed method for both adsorption and desorption branches.

traditional methods the desorption branch was chose, but in the proposed method both branches were used in order to select the most suitable for the PSD analysis of this kind of materials.

Fig. 8 shows all the PSD obtained with the methods above mentioned. As it can be observed from this figure for all samples, the PSD obtained by the new method is similar to the obtained by BJH and VBS methods in the larger mesopores and macropores region. Moreover, the only difference between these last methods is that the new developed method can detect the small mesopores (around 10 nm) which is also detected by the NLDFT method. Some important facts to highlight are: *i*) the PSD obtained with the proposed method using both branches, adsorption and desorption, give similar results in all the samples. However, in PS-HEMA and PS-MAA samples the PSD from desorption branch is placed at smaller pore sizes than those obtained with the adsorption branch, due to their hysteresis loops are wider than those of the other samples. *ii*) In PS-HEMA and PS-MAA the PSD obtained from GM/GMBET method with the adsorption branch shows a best agreement with the results of the other macroscopic methods, VBS and BJH, suggesting this branch as a good choice to evaluate the PSD in this kind of materials. *iii*) The good agreement between the BJH and VBS methods is because the overestimation in the pore size of the

BJH method is often found in samples with pore sizes smaller than 10 nm [52], and the samples present macropores. *iv*) In the case of the microscopic method NLDFT for the samples under study is not possible to see the peak corresponding to the macropores. This fact is due to the Kernel used from the desorption branch take into account relative pressure values up to 0.967 and at this point the macropores present in the samples are not filled.

Finally, for the above mentioned, the new proposed method gives suitable approximations for the PSD evaluation in materials that present isotherms type II or III. Regarding to the application range, the GM/GMBET method can be used for both branches (adsorption and desorption) within a range of relative pressures between 0.005 and 0.99 of the N_2 experimental isotherm at 77 K, taking into account the monolayer and the capillary condensation formations by applying the segmentation procedure.

Thus, this investigation leads us to demonstrate the importance of the Grand Canonical formalism in statistical mechanics where the proposed method predicts a PSD for each sample from small mesopores till larger mesopores and/or macropores. Whereas, NLDFT gives only PSD in small mesopores region and both BJH and VBS methods give only PSD in the larger mesopores and/or macropores regions.

5. Conclusion

An new method for calculating the pore size distribution is presented and validated from a comprehensive analysis of N_2 adsorption-desorption isotherms type II or III (according to IUPAC classification) where the filling mechanism of the monolayer and capillary condensation are taken into consideration. This leads us to calculate PSD in the range of small mesopores and larger mesopores and/or macropores by segmentation procedure and especially thanks to the statistical mechanics approach. The PSD obtained for the polymer latex shows that these samples are highly meso-macroporous, with only a small contribution of small mesopores (around of 10 nm). These small mesopores can be attributed to the intraparticle porosity. By using the α_s–*plot* method the absence of micropores in all samples under study was found. The difference between the obtained PSD in the macropores region was attributed to particle size of the samples under study. Furthermore, the copolymerization plays an important role in the porosity and the specific surface area, whereas the higher polydispersity index (polydisperse latex) can reduce the porosity (pore volume) by the addition of small grains within the pores placed between larger ones.

The comparison of the new proposed method with BJH, VBS and NLDFT methods, with the samples under study, leads us to conclude that the proposed method can reproduce all results found by the previous methods where some of them can be applied only for a porosity specific range. Therefore, the development of new theoretical approach has led to a better understanding of nitrogen adsorption processes onto latex particles and such robust approach can adequately cover the broad relative pressure range.

By using the segmentation procedure there is a good chance to improve the fit partially, it is always accompanied by losing a quality of the fit in other regions. Moreover, statistical mechanics formalism has the advantage of providing physical meaning to the model parameters and then a bimodal distribution is well developed for all studied samples.

References

[1] T. Suzawa, H. Shirahama, T. Fujimoto, J. Colloid Interface Sci. 86 (1982) 144–150.
[2] M. Jozefowicz, J. Jozefonvicz, Biomaterials 18 (1997) 1633–1644.
[3] J.-H. Kim, J.-Y. Yoon, in: A. Hubbard (Ed.), Encyclopedia of Surface and Colloidal Science, Marcel Dekker, New York, 2002, pp. 4373–4381.
[4] H. Shirahama, T. Suzawa, Colloid. Polym. Sci. 263 (1985) 141–146.
[5] M. Tsyurupa, V. Davankov, React. Funct. Polym. 66 (2006) 768–779.
[6] S. Gregg, K. Sing, Adsorption, Surface Area and Porosity, Academic, New York, 1982.
[7] F. Rouquerol, J. Rouquerol, K. Sing, Adsorption by Powders and Porous Solids: Principles, Methodology and Applications, Academic Press, London, 1999.
[8] C.M. Lastoskie, K.E. Gubbins, Adv. Chem. Eng. 28 (2001) 203–250.
[9] L.D. Gelb, K. Gubbins, Langmuir 15 (1999) 305–308.
[10] M. Maddox, J. Olivier, K. Gubbins, Langmuir 13 (1997) 1737–1745.
[11] C.M. Lastoskie, K.E. Gubbins, Stud. Surf. Sci. Catal. 128 (2000) 41–50.
[12] P.I. Ravikovitch, G.L. Haller, A.V. Neimark, Adv. Colloid Interface Sci. 76 (1998) 203–226.
[13] A.V. Neimark, P.I. Ravikovitch, Stud. Surf. Sci. Catal. 128 (2000) 51–60.
[14] A.C. Mitropoulos, J. Colloid Interface Sci. 317 (2008) 643–648.
[15] E.P. Barrett, L.G. Joyner, P.P. Halenda, J. Am. Chem. Soc. 73 (1951) 373–380.
[16] C. Pierce, J. Phys. Chem. 57 (1953) 149–152.
[17] D. Dollimore, G. Heal, J. Colloid Interface Sci. 33 (1970) 508–519.
[18] M. Kruk, M. Jaroniec, A. Sayari, Langmuir 13 (1997) 6267–6273.
[19] J. Villarroel-Rocha, D. Barrera, K. Sapag, Microporous Mesoporous Mater 200 (2014) 68–78.
[20] J. Villarroel-Rocha, D. Barrera, K. Sapag, Top. Catal. 54 (2011) 121–134.
[21] L. Couture, R. Zitoun, Physique Statistique, Ellipses, France, Paris, 1992.
[22] B. Diu, C. Guthmann, D. Lederer, B. Roulet, Physique Statistique, Hermann, Paris, 1989.
[23] M. Beragoui, C. Aguir, M. Khalfaoui, E. Enciso, M.J. Torralvo, L. Duclaux, L. Reinert, M. Vayer, A.B. Lamine, Progr. Theor. Exp. Phys. 2015 (2015), 033J001.
[24] M. Khalfaoui, M. Baouab, R. Gauthier, A. Ben Lamine, J. Colloid Interface Sci. 296 (2006) 419–427.
[25] M. Khalfaoui, A.E. Ghali, C. Aguir, Z. Mohamed, M.H.V. Baouab, A.B. Lamine, Ind. Crops Prod. 67 (2015) 169–178.
[26] M. Khalfaoui, S. Knani, M. Hachicha, A.B. Lamine, J. Colloid Interface Sci. 263 (2003) 350–356.
[27] M. Khalfaoui, A. Nakhli, C. Aguir, A. Omri, M. M'henni, A.B. Lamine, Environ. Sci. Pollut. Res. 21 (2014) 3134–3144.
[28] A. Nakhli, M. Bergaoui, M. Khalfaoui, J. Möllmer, A. Möller, A.B. Lamine, Adsorption 20 (2014) 987–997.
[29] J. Rouquerol, F. Rouquerol, P. Llewellyn, G. Maurin, K.S. Sing, Adsorption by Powders and Porous Solids: Principles, Methodology and Applications, Academic press, San Diego, 2013.
[30] M.C. Carbajo, E. Climent, E. Enciso, M.J. Torralvo, J. Colloid Interface Sci. 284 (2005) 639–645.
[31] A. Herzog Cardoso, C.A.P. Leite, M.E.D. Zaniquelli, F. Galembeck, Colloids Surf. A 144 (1998) 207–217.
[32] M.C. Carbajo, A. Gómez, M.J. Torralvo, E. Enciso, J. Mater. Chem. 12 (2002) 2740–2746.
[33] E. Unzueta, J. Forcada, Polymer 36 (1995) 1045–1052.
[34] M. Beragoui, C. Aguir, M. Khalfaoui, E. Enciso, M.J. Torralvo, L. Duclaux, L. Reinert, M. Vayer, A.B. Lamine, J. Appl. Polym. Sci. 132 (2015), 1097–4628.
[35] S. Brunauer, P.H. Emmett, E. Teller, J. Am. Chem. Soc. 60 (1938) 309–319.
[36] J. Rouquerol, P. Llewellyn, F. Rouquerol, Stud. Surf. Sci. Catal. (2007) 49–56.
[37] A. Sayari, P. Liu, M. Kruk, M. Jaroniec, Chem. Mater 9 (1997) 2499–2506.
[38] M. Jaroniec, M. Kruk, J.P. Olivier, Langmuir 15 (1999) 5410–5413.
[39] A. Okhovat, A. Ahmadpour, Adsorpt. Sci. Technol. 30 (2012) 159–170.
[40] L. Wang, S. Régnier, Modell. Simul. Mater. Sci. Eng. 23 (2015), 015001.
[41] J. Villarroel-Rocha, D. Barrera, A.A.G. Blanco, M.E.R. Jalil, K. Sapag, Adsorpt. Sci. Technol. 31 (2013) 165–184.
[42] M. Thommes, Chem. Ing. Tech. 82 (2010) 1059–1073.
[43] P. Tarazona, Phys. Rev. A 31 (1985) 2672.
[44] K.S. Sing, Pure Appl. Chem. 57 (1985) 603–619.
[45] A. Nakhli, M. Khalfaoui, C. Aguir, M. Bergaoui, M.F. M'henni, A. Ben Lamine, Sep. Sci. Technol. 49 (2014) 2525–2533.
[46] J. Sun, Carbon 40 (2002) 1051–1062.
[47] L. Chan, W. Cheung, S. Allen, G. McKay, Chin. J. Chem. Eng. 20 (2012) 535–542.
[48] A. Kapoor, R. Yang, Gas. Sep. Purif. 3 (1989) 187–192.
[49] J. Nimmo, Encycl. Soils Environ. 3 (2004) 295–303.
[50] B. Huang, C.H. Bartholomew, B.F. Woodfield, Microporous Mesoporous Mater 184 (2014) 112–121.
[51] P. Ravikovitch, D. Wei, W. Chueh, G. Haller, A. Neimark, J. Phys. Chem. C 101 (1997) 3671–3679.
[52] M. Thommes, Nanoporous Mater. Sci. Eng. 11 (2004) 317.